Metals and Materials International (2024) 30:1242–1255
https://doi.org/10.1007/s12540-023-01564-x

Thermodynamics of Liquid Alloys and Vapor–Liquid Equilibrium in the Antimony–Tellurium System

Valeriy Volodin[1] · Sergey Trebukhov[1] · Alina Nitsenko[1] · Xeniya Linnik[1] · Azamat Tulegenov[1]

Received: 26 June 2023 / Accepted: 26 October 2023 / Published online: 4 January 2024

Abstract

The partial and integral thermodynamic functions of formation and evaporation of antimony-tellurium melts were calculated based on the vapor pressure values of the components in the Sb–Sb_2Te_3 and Sb_2Te_3–Te systems. It is shown that integral functions of evaporation enthalpy and entropy insignificantly change in value from the alloy corresponding to the Sb_2Te_3 composition and slightly decrease in the direction of antimony and tellurium on the state diagram. However, they can be described by a linear dependence in the entire concentration interval of solutions existence within the experiment error. The boundaries of liquid and vapor coexistence fields at atmospheric pressure (101.3 kPa) and in vacuum (0.9 kPa) were calculated based on the partial pressure values of melt components. It is shown that the separation of antimony alloys with tellurium by distillation into elements at atmospheric pressure is difficult because of high boiling temperatures of antimony-based alloys. It would require a significant number of condensate re-evaporation cycles in a vacuum. The results aim at creating the fundamental physical and chemical foundations of the distillation technologies for processing melted chalcogenide systems. The second aim is to issue effective practical recommendations necessary for developing and improving the process of extracting rare metals from polymetallic mattes by vacuum-thermal method.

Keywords Entropy · Enthalpy · Vapor pressure · Melt · Vapor–liquid equilibrium

1 Introduction

In the pyrometallurgical processing of sulfide concentrates at copper, lead and antimony plants, polymetallic mattes—chalcogenide alloys—are obtained as an intermediate product. The basis of polymetallic matte copper and lead plants are copper sulfides (Cu_2S) and iron (FeS). Technologies for the production and processing of polymetallic mattes are well studied and developed. However, due to the involvement in the processing of new types of raw materials, including those poor in terms of the main component, work on their improvement is still underway [1–13].

In addition to the main components, the matte contains rare elements: cadmium, antimony, arsenic, indium, and others (in sulfide form), as well as selenium and tellurium, isomorphically replacing sulfur in sulfides [14–17]. Impurities of antimony and arsenic sulfides, selenides and tellurides in matte significantly complicate the production of high-grade copper and, besides, rare elements themselves are valuable for radioelectronic industry. In this regard, various methods intended to extract these compounds from the matte melt were and are developed now. Distillation of volatile compounds in vacuum at high temperature is one of them.

Behavior and distribution of rare element sulfides in the matte distillation in a vacuum based on a very large number of studies and technological tests are given and analyzed in [18]. A much smaller number of publications, including [19–26] devoted to the thermodynamics study of chalcogenides and double melts of rare element chalcogenides [27–31] applied to the matte processing conditions.

✉ Alina Nitsenko
alina.nitsenko@gmail.com

Valeriy Volodin
volodinv_n@mail.ru

Sergey Trebukhov
s.trebukhov@satbayev.university

Xeniya Linnik
xenija_linnik@mail.ru

Azamat Tulegenov
azamattulegenov2001@gmail.com

[1] Laboratory of Vacuum Processes, Institute of Metallurgy and Ore Beneficiation, Satbayev University, Shevchenko Str. 29/133, 050010 Almaty, Republic of Kazakhstan

Technological studies, in addition to those specified in [1] are limited with [32, 33]. In [32] the authors studied the behavior of rare metals at 1200 °C and pressure of 65 Pa and found that the antimony content did not exceed 0.1% after copper matte distillation. In the study [33] the impurities were distilled at 1100–1300 °C and pressure of 50–130 Pa. Distillation degree after processing for 40–60 min was, wt%: bismuth—88–98; antimony—40–92. Decomposition of jemsonite ($Pb_4FeSb_6S_{14}$) [34] at 700 and 900 °C in vacuum allowed to isolate up to 98% of antimony trisulfide with content of 99.17 of the main compounds.

The number of publications dedicated to thermodynamics of liquid antimony-tellurium system alloys is limited with works [19, 35–37]. In Ettler et al. [17] the antimony-tellurium mixing enthalpy (− 9.6 kJ/mol) at 935 K was determined by calorimetric method, in Singh et al. [35] the molar volumes were determined experimentally depending on temperature and composition, the presence of stable Sb_2Te_3 associates in the melt was established. In [36] also noted the congruent nature of the antimony trisulfide melting. Based on the calculation of the phase diagram by CALPAD method the authors of Guo et al. [37] determined the mixing enthalpy at 911 and 935 K, the activities of the components at 911 and 1023 K, and the Gibbs energy at 911 K which coincided well with the available experimental data.

There are no data on vapor–tellurium equilibrium in the antimony-tellurium system that allow to estimate the behavior of elements and Sb_2Te_3 compound under conditions of chalcogenide melt distillation reprocessing, as well as separation of Sb–Te melts into components.

Thermodynamic functions of melt formation and evaporation were determined, and the liquid–vapor phase transition boundaries of the Sb–Te system were calculated to compensate the missing data.

The obtained results will supplement the thermodynamic database. They can be used as reference data in physical chemistry and by technologists working in research and educational institutions of related profiles. Also, the results can be usable in developing efficient technologies for producing semiconductor tellurium and developing new environmentally friendly methods for high-purity element production from secondary products.

Table 1 Composition of alloys of the Sb–Te system

Alloy number	wt%		at%	
	Te	Sb	Te	Sb
1	13.88	86.12	13.33	86.67
2	25.59	74.41	24.71	75.29
3	36.26	63.74	35.18	64.82
4	50.28	49.72	49.11	50.89
5	61.12	38.88	60.00	40.00
6	68.87	31.13	67.86	32.14
7	76.14	23.86	75.28	24.72
8	84.31	15.69	83.68	16.32
9	91.34	8.66	90.96	9.04

2 Experimental Part

The determination of partial and integral thermodynamic functions of mixing and evaporation of antimony alloys with tellurium is based on the values of the saturated vapor pressure of the components that make up the system.

2.1 Preparation of Antimony Alloys with Tellurium

Alloys were prepared for the experiments by melting appropriate amounts of antimony and tellurium in quartz ampoules, from which air was evacuated before sealing. To prepare the alloys, elemental tellurium and antimony were used, each containing more than 99.99 wt% of the main element. The temperature was raised by 100 K above the liquidus line and kept at this temperature for 12 h. At the end of the exposure, the ampoules with the alloy were quenched in water. The compositions of the obtained alloys are shown in Table 1.

The congruent melting of Sb_2Te_3 [36], as well as the presence of stable associates Sb_2Te_3 in the melt [35] allows us to consider this compound as a separate substance with a fixed melting point (891 K), and the antimony–tellurium diagram as two particular ones: Sb–Sb_2Te_3 и Sb_2Te_3–Te.

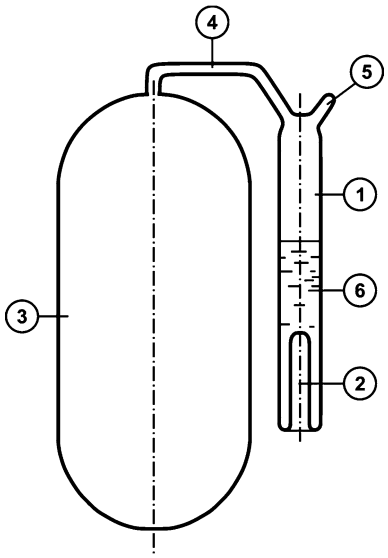

Fig. 1 Scheme of a vessel for determining the composition of vapor by a static method: (1) ampoule for the alloy; (2) socket for thermocouple; (3) ampoule for vapor; (4) capillary; (5) process for introducing the alloy; (6) alloy

2.2 Saturated Vapor Pressure Determination

Due to the fact that the saturation vapor pressure Sb, Sb_2Te_3 and Te under equal conditions comparable in magnitude and all of them are present in the vapor phase, first, the molar fraction in the vapor phase of the most volatile component was experimentally determined: Sb_2Te_3 in system Sb–Sb_2Te_3 and Te in system Sb_2Te_3–Te. Then, by multiplying the total pressure over the melt by the mole fraction of the more volatile component in the vapor phase, we calculated the partial pressure of the saturated vapor of the more volatile component over the melt in each of the particular systems. The saturation vapor pressure of the less volatile component was calculated by numerical integration of the Gibbs–Duhem equation.

2.2.1 Determination of a Vapor Composition

The proportion of Sb_2Te_3 in the Sb–Sb_2Te_3 system and Te in the Sb_2Te_3– Te system was determined by a static method using a vessel made of quartz glass, the scheme of which is shown in Fig. 1. The vessel consists of two ampoules connected by a capillary: small *(1)*–to accommodate a sample alloy, large *(3)*–for the vapor phase in equilibrium with the alloy. Pre-set time to reach equilibrium.

The experimental procedure was as follows. A weighed portion of the alloy under study was loaded into the ampoule for the alloy *(1)* through the filling process *(5)*. The vessel was washed three times with argon and pumped out to a pressure of 1 Pa, after which the offshoot was sealed off. The vessel prepared in this way was placed in the isothermal zone of the furnace, heated to a temperature of 1173 and 1373 K for alloys of the Sb–Sb_2Te_3 system, and to 973 and 1173 K for alloys of the Sb_2Te_3–Te system, and kept for 24 h. After the exposure time, the vessel was removed and quenched in water. The ampoule with the vapor phase condensate *(3)* was cut off. The vapor condensate was dissolved in it and analyzed. The number of elements in the solution was determined on an atomic absorption spectrophotometer. In this case, the amount of tellurium in the condensate for the Sb–Sb_2Te_3 system and the amount of antimony in the condensate in the Sb_2Te_3–Te system were considered to belong to antimony telluride.

2.2.2 Determination of the Total Vapor Pressure by the Boiling Points Method

The boiling point method was used to determine the total pressure. It is based on a significant increase in the evaporation rate when the external pressure and the saturated vapor pressure of the test substance are equal with a decrease in pressure over the melt at a given temperature.

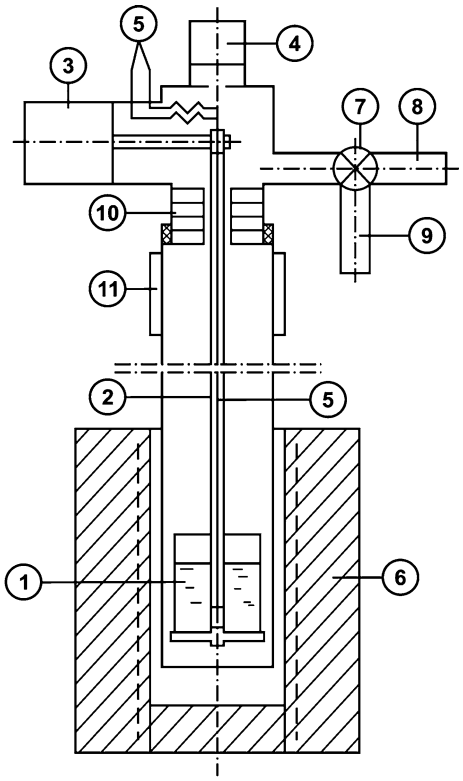

Fig. 2 Scheme of the installation for determining the vapor pressure: (1) crucible; (2) suspension; (3) weight measurement system; (4) pressure measurement system; (5) thermocouple; (6) electric furnace; (7) leak valve; (8) gas evacuation channel; (9) inert gas supply channel; (10)shield; (11) caisson

The installation scheme for determining the vapor pressure by the boiling point method is shown in Fig. 2.

The installation is a retort made of two parts: the lower one, placed in an electric furnace *(6)* with automatic temperature maintenance, and the upper one, made of quartz glass. Inside the retort on a hollow suspension *(2)* there is a crucible *(1)* with a sample of the alloy. Inside the suspension, at the level of the melt in the crucible, there is a junction of a platinum-platinum–rhodium thermocouple *(5)*.

The suspension rests on the scales of the mass loss measurement system *(3)* located in the upper part of the retort. The parts of the retort are articulated using a rubber seal removed from the high temperature zone. The lower and upper parts of the retort are separated by screens *(10)* to reduce the heat flow from the high temperature zone. In the upper part of the retort, there is a pressure measurement system *(4)*, channels for gas evacuation *(8)*, filling with argon *(9)*, and exits of the thermocouple ends *(5)*. Systems for measuring weight loss *(3)*, pressure *(4)*, temperature *(5)* have a signal output to a multipoint potentiometer with measurement fixation on a chart tape.

The experimental procedure was as follows. A portion of the alloy (up to 2 g) was placed in a crucible, which was mounted on a suspension with the retort disconnected outside the heating zone. Then the lower part of the retort was articulated with the upper one. Gases were evacuated from the retort twice with a vacuum pump and then filled the retort with argon. After that, the lower part of the retort was placed in the isothermal zone of the preheated electric furnace. The retort was heated at an excess pressure of 2–5 kPa with an open inert gas supply system to suppress the evaporation process of the components and compensate for the pressure increase in the retort due to gas expansion during heating. When the weighed portion of the alloy reached the predetermined temperature, the evacuation of argon from the volume of the retort was started while maintaining a constant temperature of the alloy (isothermal version). At the same time, the weight loss of the sample (Δm) and the change in pressure (P) were synchronously recorded.

The pressure at which a sharp increase in the evaporation rate was observed (a break in the curve of the dependence of the change in mass loss on pressure) was considered equal to the total vapor pressure over the alloy. The numerical value of the vapor pressure (P) was determined by the joint solution of equations describing the dependence $P = f(\Delta m)$ before and after the observed break on the curve describing the experimental data.

2.3 Calculation of the Boundaries of the Field of Coexistence of Liquid and Vapor

The vapor–liquid equilibrium data are of paramount importance for the development and optimization of parameters for the main separation processes in chemical and metallurgical technology, first and foremost in distillation processes.

Such studies of systems containing chalcogenes and chalcogenides are difficult because of high boiling temperatures of solutions, the difficulty to determine the concentration of components in the vapor phase in equilibrium with the alloy and the problem of instrumental design of ebuliometric measurements due to the vapor aggressiveness to the materials of equipment.

Because there is no boiling process for liquid chalcogenide solutions due to the high density of their constituents, the boiling temperature was determined equal to the temperature at which the sum of the partial pressures of the system components according to Dalton's law, was equal to atmospheric (101.3 kPa) or another pressure corresponding to the vacuum technology conditions. Thus, temperature-concentration dependences for partial pressures of elements and compounds were required for calculation of phase boundaries.

The vapor phase composition (concentration of antimony (y_{Sb}) and Sb_2Te_3 ($y_{Sb_2Te_3}$)) over Sb–Sb_2Te_3 melts at boiling point was determined as:

$$y_{Sb}(y_{Sb_2Te_3})\,[\text{mole fraction}] = n_{Sb}(n_{Sb_2Te_3})/(n_{Sb} + n_{Sb_2Te_3}) = \bar{p}_{Sb}(\bar{p}_{Sb_2Te_3})/(\bar{p}_{Sb} + \bar{p}_{Sb_2Te_3}) \quad (1)$$

where n_{Sb} and $n_{Sb_2Te_3}$—number of antimony and telluride moles in the vapor phase; $\overline{p}_{Sb}$ and $\overline{p}_{Sb_2Te_3}$—partial pressures of antimony and antimony telluride vapor, Pa.

The vapor phase composition (concentration of antimony telluride ($y_{Sb_2Te_3}$) and tellurium (y_{Te})) over Sb_2Te_3–Te melts was determined as:

$$y_{Sb_2Te_3}\,(y_{Te})[\text{mole fraction}] = n_{Sb_2Te_3}(n_{Te})/(n_{Sb_2Te_3} + n_{Te}) = \bar{p}_{Sb_2Te_3}(\bar{p}_{Te})/(\bar{p}_{Sb_2Te_3} + \bar{p}_{Te}) \quad (2)$$

where $n_{Sb_2Te_3}$ and n_{Te}– number of telluride and tellurium moles in the vapor phase; $\overline{p}_{Sb_2Te_3}$ и $\bar{p}_{Te}$—partial pressures of antimony telluride and tellurium vapor in the vapor phase, Pa.

When liquid–vapor phase transition is made, it is important to evaluate the effect of pressure reduction within one atmosphere on the temperature of condensed phase transitions. The authors [38] established the dependence of the liquidus temperature on pressure when the cadmium-lead diagram was studied and the pressure was increased up to 4GPa. When the pressure was changed with the transition to vacuum (at 0.1 MPa) melting temperature could be reduced by $5.6 \cdot 10^{-3}$ K. That is, low pressure has almost no effect on the temperature of phase transitions of condensed systems, and it was not taken into account when the diagram was constructed.

The correctness of determination of the boiling point for solutions—melts, and the vapor phase composition is confirmed by the authors on the example of the cadmium-zinc system [39] where the results of direct measurements of the boiling point and vapor composition [40, 41] practically coincided with our results.

3 Results and Discussion

3.1 Saturated Vapor Pressure Values for Antimony and Tellurium Melt Components

3.1.1 Composition of the Vapor Phase in the Sb–Te System

Based on experimental data on the mass amount of antimony, tellurium, and antimony telluride in the condensate, the molar

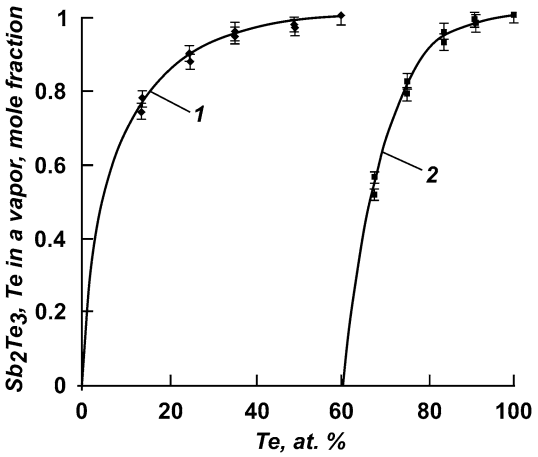

Fig. 3 Contents of antimony telluride (1) and tellurium (2) in a vapor

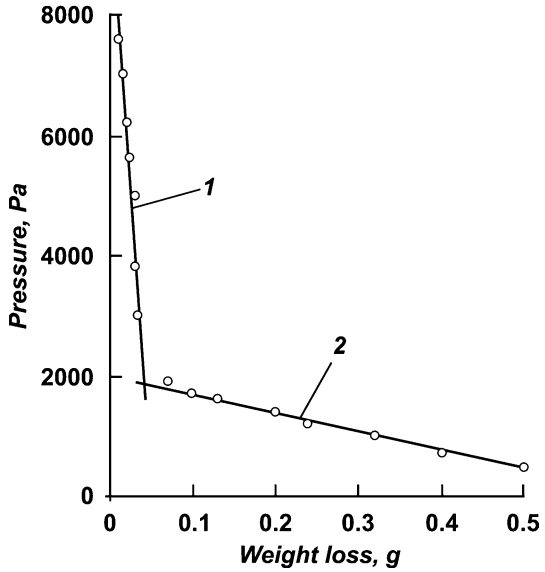

Fig. 4 Changes in the alloy mass loss (alloy 6) with pressure decrease: (1) before boiling point; (2) after boiling point

ratio of elements and Sb_2Te_3 in the vapor phase was calculated (Fig. 3). Figure 3 shows the concentration of tellurium in the starting alloy on the abscissa. The ordinate axis shows the content of antimony telluride for the concentration range in the starting alloy 0–60 at% for the particular system Sb–Sb_2Te_3. This axis also shows the tellurium content for the particular system Sb_2Te_3–Te at 60–100 at% Te in the starting alloy. This is because, in the first concentration range, the vapor phase is represented by antimony and tellurium and antimony compounds that total the composition of Sb_2Te_3. In the second concentration range of the starting alloys, tellurium and Sb_2Te_3 represent the vapor.

Due to the fact that the results of the vapor composition determination in the temperature range equal to 200 K had a difference within the experiment error, the content of antimony telluride and tellurium in the vapor phase is approximated by each one dependence Eqs. (3), (4). The representation of the dependences of vapor pressure values on the composition of the initial alloy by fourth-order polynomials is because this allows, on the one hand, to correctly describe complex concentration dependences (errors in approximation of experimental data). On the other hand, and most importantly, it makes it possible to perform numerical integration of these dependencies when calculating thermodynamic functions using the Gibbs–Duhem equation of the second component of the system. When describing experimental data by other methods, thermodynamic functions are calculated graphically. This complicates the calculations and reduces their accuracy.

The content of antimony telluride in the vapor phase ($Y_{Sb_2Te_3}$) over Sb–Sb_2Te_3 liquid solutions corresponded to the dependence:

$$Y_{Sb_2Te_3}[\text{mole.fraction}] = -4.214x^4_{Sb_2Te_3} + 11.727x^3_{Sb_2Te_3} - 11.925x^2_{Sb_2Te_3} + 5.412x_{Sb_2Te_3} \quad (3)$$

where $x_{Sb_2Te_3}$—is a molar fraction of telluride in the alloy of the Sb–Sb_2Te_3 specific system, provided that $x_{Sb_2Te_3} + x_{Sb} = 1$ (x_{Sb} is a mole fraction of antimony in the alloy). The approximation error is 2.08%.

The tellurium content in the vapor phase (Y_{Te}) over Sb_2Te_3–Te liquid solutions corresponds to the equation:

$$Y_{Te}[\text{mole.fraction}] = -0.775x^4_{Te} + 3.18x^3_{Te} - 5.006x^2_{Te} + 3.601x_{Te} \quad (4)$$

where mole tellurium fraction in the alloy of the Sb_2Te_3–Te specific system, provided that $x_{Sb_2Te_3} + x_{Te} = 1$ ($x_{Sb_2Te_3}$—mole fraction of antimony telluride in the alloy). Approximation error is 2.29%.

3.1.2 Total Vapor Pressure over Alloys of the Sb–Te System

The calculation of the total vapor pressure (P^{tot}) is given on the example of alloy 6 (Table 1), which contains 67.86 at% Te, at a temperature of 1073 K (Fig. 4).

As can be seen, the experimental curve is well described by first-order equations. In this case, alloy pressure and mass loss (Δm, g) before the curve break were related by dependence Eq. (5), after the break—by dependence Eq. (6).

Table 2 Results of experiments to determine the total vapor pressure of the Sb–Te system

System Sb – Sb_2Te_3				System Sb_2Te_3 – Te			
Alloy	[Te], at. %.	T,K	P^{tot}, kPa	Alloy	[Te], at. %.	T,K	P^{tot}, kPa
1	13.33	1,173	1.09	6	67.86	1,073	1.75
			1.46				1.90
			1.27				2.10
		1,373	12.57			1,273	20.55
			12.57				21.48
			13.11				21.22
2	24.71	1,173	1.77	7	75.28	1,073	3.73
			1.91				3.73
			1.91				4.13
		1,373	18.73			1,273	44.26
			19.76				45.06
			19.03				45.60
3	35.18	1,173	2.56	8	83.68	973	1.33
			2.69				1.60
			2.98				1.60
		1,373	26.84			1,173	23.20
			26.69				23.73
			27.83				23.60
4	49.11	1,173	4.08	9	90.96	973	2.27
			3.95				2.67
			4.62				2.27
		1,373	38.63			1,173	31.33
			39.18				32.26
			38.91				32.66
5	60.00	1,073	1.33	10	100	873	0.66
			1.47				0.83
			1.33				0.59
			1.73				0.54
		1,273	18.53			1,073	13.73
			18.93				14.85
			19.06				12.91
			18.66				13.44

$$P_1 = -174{,}856\Delta m + 9{,}578.8 \quad (5)$$

$$P_2 = -3{,}224\Delta m + 2{,}039.9 \quad (6)$$

The total vapor pressure for these conditions was determined to be 1,898 Pa by solving obtained equations together, and rounded down to 1.90 kPa. The dependence of the mass loss with pressure decrease at the boiling point might have a less significant kink. In such a case, the curve sections adjacent to the kink were approximated by second-order equations.

The calculated values of the total vapor pressure over alloys of the Sb–Te system are shown in Table 2.

3.1.3 Saturated Vapor Pressure of Liquid Alloy Components

Determination of saturated vapor pressure values for components of liquid alloys is given on the example of the system Sb–Sb_2Te_3, and was as follows.

Partial vapor pressure of more volatile antimony telluride ($\overline{p}_{Sb_2Te_3}$) was calculated by the product of the total vapor pressure (P^{tot}), found experimentally, by the mole fraction of Sb_2Te_3 in the vapor phase ($Y_{Sb_2Te_3}$): $\overline{p}_{Sb_2Te_3} = P^{tot} \times Y_{Sb_2Te_3}$. Then, the equation coefficients *A* and B of the partial pressure

dependence in the form of $\ln \overline{p}_{Sb_2Te_3}[\text{Pa}] = -A \cdot T^{-1} + B$ were approximated by concentration dependences as $A = f(x_{Sb_2Te_3})$ and $B = f(x_{Sb_2Te_3})$. As a result, the temperature-concentration dependence of the partial pressure of antimony telluride in a particular system Sb–$Sb_2Te_3$was obtained:

$$\begin{aligned}\ln \overline{p}_{Sb_2Te_3} = (&21,720x^4_{Sb_2Te_3} - 59,003x^3_{Sb_2Te_3} + 58,172x^2_{Sb_2Te_3} \\ &- 22,462x_{Sb_2Te_3} - 15,894) \cdot T^{-1} - 10.68x^4_{Sb_2Te_3} \\ &+ 30.123x^3_{Sb_2Te_3} - 30.706x^2_{Sb_2Te_3} + 12.095x_{Sb_2Te_3} \\ &+ 22.731 + \ln x_{Sb_2Te_3}\end{aligned} \tag{7}$$

where $x_{Sb_2Te_3}$–mole fraction of antimony telluride, on condition that $x_{Sb_2Te_3} + x_{Sb} = 1$ (x_{Sb}–mole fraction of antimony in the alloy).

The antimony telluride activity ($a_{Sb_2Te_3}$) under the same condition was found as the ratio of the Sb_2Te_3 partial pressure to the total pressure above the solution: $a_{Sb_2Te_3} = \overline{p}_{Sb_2Te_3}/P^{tot}$ and was represented by the expression:

$$\begin{aligned}\ln a_{Sb_2Te_3} =&(21,720x^4_{Sb_2Te_3} - 59,003x^3_{Sb_2Te_3} + 58,172x^2_{Sb_2Te_3} \\ &- 22,462x_{Sb_2Te_3} + 1,573) \cdot T^{-1} - 10.68x^4_{Sb_2Te_3} \\ &+ 30.123x^3_{Sb_2Te_3} - 30.706x^2_{Sb_2Te_3} + 12.095x_{Sb_2Te_3} \\ &- 0.832 + \ln x_{Sb_2Te_3}\end{aligned} \tag{8}$$

Accordingly, the antimony telluride activity coefficient ($\gamma_{Sb_2Te_3}$) was equal to $\gamma_{Sb_2Te_3} = \overline{p}_{Sb_2Te_3}/(P^{tot} \times x_{Sb_2Te_3})$ and has the form:

$$\begin{aligned}\ln \gamma_{Sb_2Te_3} =&(21,720x^4_{Sb_2Te_3} - 59,003x^3_{Sb_2Te_3} + 58,172x^2_{Sb_2Te_3} \\ &- 22,462x_{Sb_2Te_3} + 1,573) \cdot T^{-1} - 10.68x^4_{Sb_2Te_3} \\ &+ 30.123x^3_{Sb_2Te_3} - 30.706x^2_{Sb_2Te_3} + 12.095x_{Sb_2Te_3} \\ &- 0.832\end{aligned} \tag{9}$$

The saturated antimony vapor pressure ($\overline{p}_{Sb}$) in the system Sb–Sb_2Te_3 was calculated by multiplying the vapor pressure over elemental antimony (p^o_{Sb}) by its activity in solution: (a_{Sb}): $\overline{p}_{Sb} = p^o_{Sb} \times a_{Sb}$ or $\overline{p}_{Sb} = p^o_{Sb} \times \gamma_{Sb} \times x_{Sb}$, where γ_{Sb} is the antimony activity coefficient under the condition that $x_{Sb_2Te_3} + x_{Sb} = 1$.

γ_{Sb} is found by numerical integration of the Gibbs–Duhem equation using the auxiliary function $\alpha_{Sb_2Te_3} = \ln \gamma_{Sb_2Te_3}/x^2_{Sb}$, proposed by Darken, which, after transformation and substitution into Eq. (10), relates $\ln \gamma_{Sb_2Te_3}$ and $\ln \gamma_{Sb}$ in the form of expression Eq. (11), which is convenient for numerical integration.

$$\ln \gamma_{Sb} = -\int_{\ln \gamma_{Sb_2Te_3} at\ x_{Sb}=1}^{\ln \gamma_{Sb_2Te_3} at\ x_{Sb}} \frac{x_{Sb_2Te_3}}{x_{Sb}} d \ln \gamma_{Sb_2Te_3} \tag{10}$$

$$\ln \gamma_{Sb} = -\frac{\ln \gamma_{Sb_2Te_3} \cdot x_{Sb_2Te_3} \cdot x_{Sb}}{x^2_{Sb}} + \int_{x_{Sb_2Te_3}=0}^{x_{Sb_2Te_3}} \frac{\ln \gamma_{Sb_2Te_3}}{(1 - x_{Sb_2Te_3})^2} dx_{Sb_2Te_3} \tag{11}$$

The activity coefficient, activity and partial pressure of antimony vapor, found in a similar way are represented by expressions:

$$\begin{aligned}\ln \gamma_{Sb} =&(21,720x^4_{Sb} - 56,837x^3_{Sb} + 53,298x^2_{Sb} \\ &- 26,722x_{Sb} + 8,541 + 3,753 \ln x_{Sb}) \cdot T^{-1} \\ &- 10.68x^4_{Sb} + 26.837x^3_{Sb} \\ &- 23.312x^2_{Sb} + 10.502x_{Sb} - 3.347 - 1.668 \ln x_{Sb}\end{aligned} \tag{12}$$

$$\begin{aligned}\ln a_{Sb} = &(21,720x^4_{Sb} - 56,837x^3_{Sb} \\ &+ 53,298x^2_{Sb} - 26,722x_{Sb} + 8,541 \\ &+ 3,753 \ln x_{Sb}) \cdot T^{-1} - 10.68x^4_{Sb} + 26.837x^3_{Sb} \\ &- 23.312x^2_{Sb} + 10.502x_{Sb} - 3.347 - 0.668 \ln x_{Sb}\end{aligned} \tag{13}$$

$$\begin{aligned}\ln \overline{p}_{Sb} = &(21,720x^4_{Sb} - 56,837x^3_{Sb} + 53,298x^2_{Sb} \\ &- 26,722x_{Sb} - 8,214 + 3,753 \ln x_{Sb}) \cdot T^{-1} \\ &- 10.68x^4_{Sb} + 26.837x^3_{Sb} - 23.312x^2_{Sb} \\ &+ 10.502x_{Sb} + 16.961 - 0.668 \ln x_{Sb}\end{aligned} \tag{14}$$

Solution compositions expressed in terms of tellurium [Te] concentration, experiment temperature (T), the value of the total vapor pressure (P^{tot}) determined experimentally, the antimony telluride proportion in the vapor ($Y_{Sb_2Te_3}$), the antimony telluride vapor pressure value ($\overline{p}_{Sb_2Te_3}$ experiment) and the same calculated by the approximating equation ($\overline{p}_{Sb_2Te_3}$ calculation), as well as the calculated value of antimony partial vapor pressure ($\overline{p}_{Sb}$) were given in Table 3.

The partial pressure values of the Sb_2Te_3–Te specific system components were found in a similar way. Solution compositions expressed in terms of tellurium [Te] concentration, experiment temperature (T), the total vapor pressure value (P^{tot}) determined experimentally, tellurium share in vapor (Y_{Te}), the tellurium partial vapor pressure value ($\overline{p}_{Te}$, experiment.) an and the same calculated by the approximating equation ($\overline{p}_{Te}$, calculation), and the calculated value of antimony telluride partial pressure ($\overline{p}_{Sb_2Te_3}$ calculation) are given in Table 4.

The total error of the Sb–Sb_2Te_3 system, equal to 8.12, determinations was calculated as the sum of independent measurement errors, %: temperature—1; weighing—0.1; pressure—0.5; approximation of antimony telluride

Table 3 Conditions and results of experiments intended to determine the vapor pressure of $Sb–Sb_2Te_3$ system components

[Te], at. %	T,K	P^{tot}, kPa	$Y_{Sb_2Te_3}$	$\overline{p}_{Sb_2Te_3}$ experiment, kPa	$\overline{p}_{Sb_2Te_3}$ calculation, kPa	$\overline{p}_{Sb}$, kPa	Error, %
13.33	1,173	1.09	0.732	0.80	0.93	0.35	–13.98
		1.46		1.07			+15.05
		1.27		0.93			0
	1,373	12.57		9.20	9.42	2.70	–2.39
		12.57		9.20			–2.39
		13.11		9.60			+1.91
24.71	1,173	1.77	0.904	1.60	1.65	0.27	–3.03
		1.91		1.73			+4.85
		1.91		1.73			+4.85
	1,373	18.73		16.93	16.97	2.06	–0.24
		19.76		17.86			+5.24
		19.03		17.20			+1.36
35.18	1,173	2.56	0.939	2.40	2.60	0.17	–7.69
		2.69		2.53			–2.69
		2.98		2.80			+7.69
	1,373	26.84		25.20	25.51	1.37	–1.22
		26.69		25.06			–1.76
		27.83		26.13			+2.43
49.11	1,173	4.08	0.980	4.00	4.11	0.06	–2.68
		3.95		3.87			–5.84
		4.62		4.53			+10.22
	1,373	38.63		37.86	37.69	0.52	+0.45
		39.18		38.40			+1.88
		38.91		38.13			+1.17
60.00	1,073	1.33	1.0	1.33	1.46	–	–8.90
		1.47		1.47			+0.68
		1.33		1.33			–8.90
		1.73		1.73			+18.49
	1,273	18.53		18.53	18.80	–	–1.44
		18.93		18.93			+0.69
		19.06		19.06			+1.38
		18.66		18.66			–0.74
							$\lvert\Delta\rvert_{cp.}$= 4.44

content values in vapor—2.08; experimental data approximation—4.44. In the Sb_2Te_3–Te system, with an approximation error of the tellurium content in vapor equal to 2.29% and an error in the description of experimental data equal to 6.86%, the total error was 10.75%.

3.2 Thermodynamic Mixing and Evaporation Functions of Sb–Te Alloys

The integral and partial values of mixing entropies and enthalpies are calculated based on the activity values of the components composing the Sb–Te, liquid system. The activity of each component (a_i) constituting the system is related to the partial Gibbs free energy of mixing ($\Delta\overline{G}_i$) by the expression $\Delta\overline{G}_i = -RT\ln a_i$ for isobaric-isothermal conditions. And based on this expression the partial change in mixing entropy of the component is determined by differentiation ($\Delta\overline{S}_i$): $\left(\partial\Delta\overline{G}_i/\partial T\right)_P = -\Delta\overline{S}_i$ and then the partial change in the mixing enthalpy ($\Delta\overline{H}_i$): $\Delta\overline{H}_i = \Delta\overline{G}_i + T\Delta\overline{S}_i$. The integral mixing functions of the alloys are defined as the sum of the fractions of the partial mixing functions.

The partial and integral mixing functions are shown in Fig. 5.

If the dependencies are analyzed it can be seen that the integral entropy of alloy mixing in the $Sb–Sb_2Te_3$ specific system has a maximum of 4.28 ± 0.29 J/(mol × K), corresponding to the composition of 16.3 at% Te in the melt. The mixing entropy determined by us is negative in the concentration interval from 12 to 60 at% Te in relation to the ideal solution. The formation of alloys is accompanied by an increase in disorder in the system and proceeds mainly with heat release. The process of alloy formation is endothermic with enthalpy maximum of 0.50 ± 0.03 kJ/mol up to the content of about 12 at% Te in the alloy. Dependence of the mixing enthalpy on the composition from 12 to 60 at%

Table 4 Conditions and results of experiments intended to determine the vapor pressure of components in the Sb_2Te_3–Te system

[Te], at. %	T, K	P^{tot}, kPa	Y_{Te}	$\overline{p}_{Te}$, experiment, kPa	$\overline{p}_{Te}$, calculation, kPa	$\overline{p}_{Sb_2Te_3}$, kPa	Error, %
67.86	1,073	1.75	0.537	0.94	0.85	0.35	+10.59
		1.90		1.02			+20.00
		2.10		1.12			+32.76
	1,273	20.55		11.04	11.15	2.70	–0.99
		21.48		11.54			+3.50
		21.22		11.40			+2.24
75.28	1,073	3.73	0.806	3.01	3.03	0.27	–0.66
		3.73		3.01			–0.66
		4.13		3.33			+9.90
	1,273	44.26		35.66	35.32	2.06	+0.96
		45.06		36.31			+2.80
		45.60		36.74			+4.02
83.68	973	1.33	0.942	1.25	1.47	0.17	–14.97
		1.60		1.51			+2.72
		1.60		1.51			+2.72
	1,173	23.20		21.85	22.93	1.37	–4.71
		23.73		22.35			–2.53
		23.60		22.23			–3.05
90.96	973	2.27	0.985	2.23	2.39	0.06	–6.69
		2.67		2.63			+10.04
		2.27		2.23			–6.69
	1,173	31.33		30.84	31.62	0.52	–2.47
		32.26		31.76			+0.44
		32.66		32.15			+1.68
100	873	0.66	1.0	0.66	0.65	–	+1.54
		0.83		0.83			+27.69
		0.59		0.59			–9.23
		0.54		0.54			–16.92
	1,073	13.73		13.73	13.72	–	+0.07
		14.85		14.85			+8.24
		12.91		12.91			–5.90
		13.44		13.44			–2.04
							$\lvert\Delta\rvert_{average}$= 6.86

Te in the alloy has a minimum (-5.29 ± 0.36 kJ/mol) at 42.0 at% Te, i.e., the alloy formation has an exothermic character. However, a small exothermic effect value indicates a weak interaction of dissimilar particles in a liquid bath.

The changes of the integral mixing entropy in a particular Sb_2Te_3–Te system are reversible: the formation of solutions is accompanied by an increase in disorder in the system with the maximum function (1.57 ± 0.17 J/(mol × K)) in the concentration range from 60.0 to 70.6 at% Te; some ordering of particles in the melt with the function minimum (− 2.37 ± 0.25 J/(mol × K)) is observed from 70.6 to 100 at% Te. The mixing enthalpy change is negative over the entire range of existence of liquid alloys of the Sb_2Te_3–Te system with a minimum (-11.80 ± 1.27 kJ/mol) at 82.9 at% tellurium in solution. The noticeable negative value of the mixing enthalpy is a sign of exothermic process accompanied by the interaction of dissimilar particles in the liquid phase.

The partial entropies of the melt component evaporation: antimony ($\Delta\overline{S}^V_{Sb}$), antimony telluride ($\Delta\overline{S}^V_{Sb_2Te_3}$), and tellurium ($\Delta\overline{S}^V_{Te}$) were found by differentiation of the partial Gibbs evaporation energy that is equal to $\Delta\overline{G}^V_{Sb(Sb_2Te_3,Te)} = -RT\ln\overline{p}_{Sb\,(Sb_2Te_3,Te)}$ where $\overline{p}_{Sb}$,$\overline{p}_{Sb_2Te_3}$,$\overline{p}_{Te}$ are the partial pressures of the components above the melt. The partial enthalpies of evaporation were found as $\Delta\overline{H}_{Sb\,(Sb_2Te_3,Te)} = \Delta\overline{G}^V_{Sb\,(Sb_2Te_3,Te)} + T\Delta\overline{S}_{Sb\,(Sb_2Te_3,Te)}$.

Integral thermodynamic functions of evaporation were calculated as the sum of fractions of partial ones.

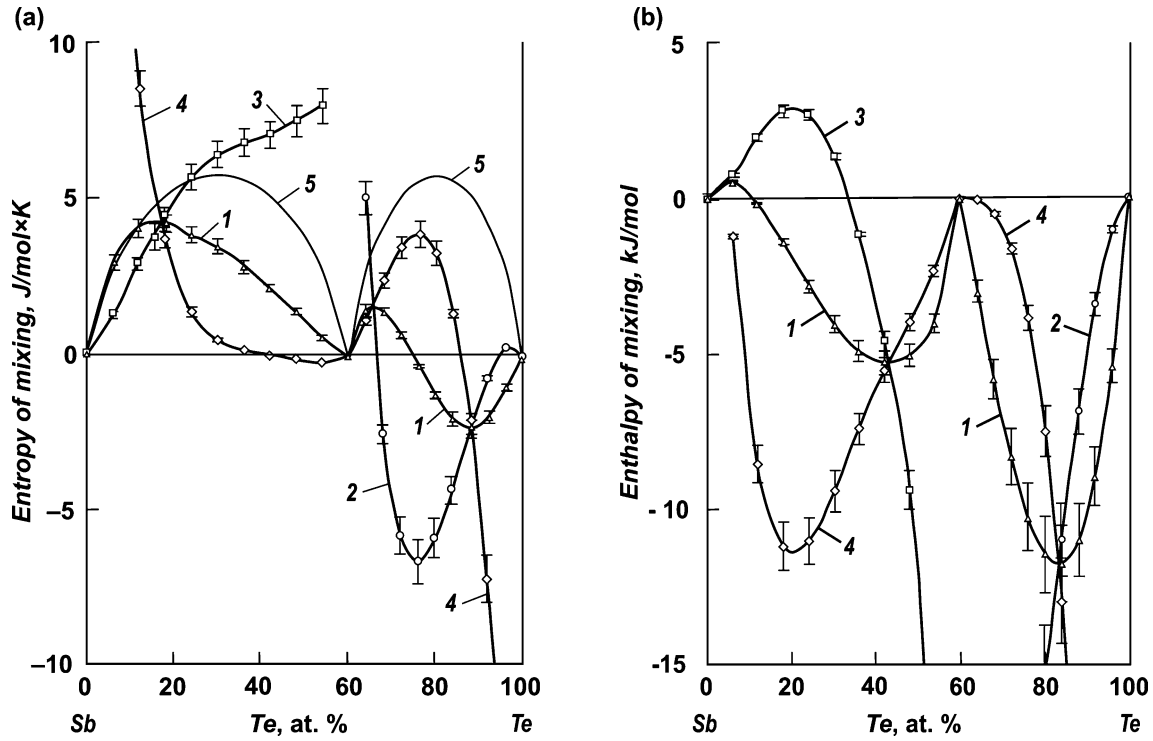

Fig. 5 Integral (1, 5) and partial (2–4) entropy **a** and enthalpy **b** functions of antimony – tellurium melts: (2) tellurium; (3) antimony; (4) antimony telluride; (5) ideal system

Table 5 Partial and integral entropies of the Sb–Te system evaporation

Alloy composition, at%		$\Delta\overline{S}^{V}_{Te}$ (J/(mol×K))	$\Delta\overline{S}^{V}_{Sb_2Te_3}$ (J/(mol×K))	$\Delta\overline{S}^{V}_{Sb}$, J/(mol×K)	ΔS^{V}_{Sb-Te} (J/(mol×K))
Te	Sb				
0	100	–	–	73.02 ± 5.93	73.02 ± 5.93
10	90	–	89.03 ± 7.23	70.67 ± 5.74	73.33 ± 5.95
20	80	–	97.36 ± 7.90	68.08 ± 5.53	77.84 ± 6.32
30	70	–	99.61 ± 8.09	66.58 ± 5.41	83.10 ± 6.75
40	60	–	100.03 ± 8.12	66.03 ± 5.36	88.70 ± 7.20
50	50	–	100.27 ± 8.14	65.27 ± 5.30	94.43 ± 7.67
60	40	–	100.08 ± 8.13	–	100.08 ± 8.13
70	30	123.74 ± 13.30	97.10 ± 10.44	–	103.77 ± 11.15
80	20	125.11 ± 13.45	96.77 ± 10.40	–	110.95 ± 11.93
90	10	120.70 ± 12.98	104.63 ± 11.25	–	116.69 ± 12.54
100	0	119.19 ± 12.81	–	–	119.19 ± 12.81

Values of changes in partial and integral entropy of evaporation depending on solution composition are given in Table 5, in enthalpy in Table 6.

The partial entropy value of antimony evaporation ($\Delta\overline{S}^{V}_{Sb}$) in the Sb–$Sb_2Te_3$ specific system does not exceed the value of 73.02 ± 5.93 J/(mol × K) which indicates the presence of associates in the vapor phase in accordance with the Trouton's rule. The partial contribution $\Delta\overline{S}^{V}_{Sb}$ has a marked effect on the integral entropy value of evaporation (ΔS^{V}_{Sb-Te}) of antimony melts at the state diagram edge. The integral enthalpy and entropy functions of evaporation decrease insignificantly in value from the alloy corresponding to the Sb_2Te_3 composition towards antimony and tellurium on the state diagram, however, they may be described by a linear dependence within the entire concentration interval of solution existence, within the limits of experimental error.

Table 6 Partial and integral enthalpies of the Sb–Te system evaporation

Alloy composition, at%		$\Delta\overline{H}^{V}_{Te}$ (kJ/mol)	$\Delta\overline{H}^{V}_{Sb_2Te_3}$ (kJ/mol)	$\Delta\overline{H}^{V}_{Sb}$ (kJ/mol)	ΔH^{V}_{Sb-Te} (kJ/mol)
Te	Sb				
0	100	–	–	139.31 ± 11.31	139.31 ± 11.31
10	90	–	151.99 ± 12.34	137.78 ± 11.19	140.15 ± 11.38
20	80	–	156.60 ± 12.72	136.46 ± 11.08	143.17 ± 11.63
30	70	–	154.65 ± 12.56	138.01 ± 11.21	146.33 ± 11.88
40	60	–	151.37 ± 12.29	142.68 ± 11.58	148.47 ± 12.06
50	50	–	148.71 ± 12.07	150.95 ± 12.26	149.09 ± 12.11
60	40	–	145.22 ± 11.79	–	145.22 ± 11.79
70	30	144.65 ± 15.55	146.18 ± 15.71	–	145.80 ± 15.67
80	20	134.37 ± 14.44	152.72 ± 16.42	–	143.54 ± 14.32
90	10	124.02 ± 13.33	170.63 ± 18.34	–	135.67 ± 14.58
100	0	118.96 ± 12.91	–	–	118.96 ± 12.91

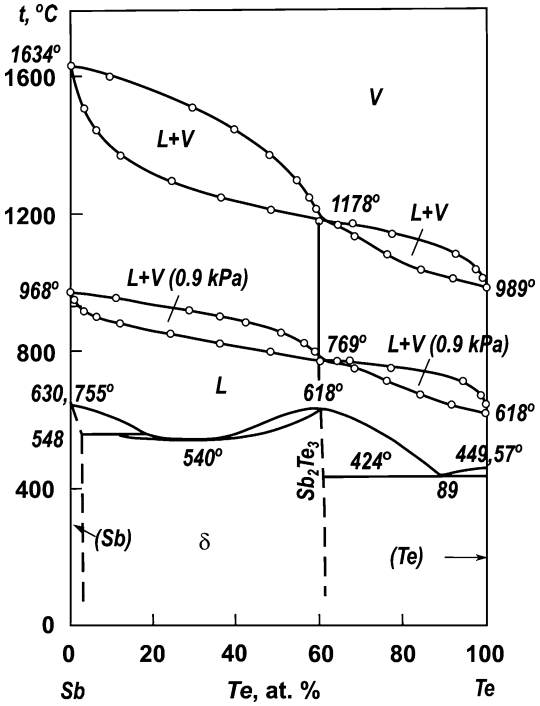

Fig. 6 Phase diagram of antimony–tellurium system

The calculated values make it possible to determine the energy costs of distillation separation for liquid alloys of the antimony–tellurium system.

3.3 Phase Transition Liquid–Vapor in the Antimony–Tellurium System

Based on the temperature-concentration dependences of the partial pressure values of the saturated vapor of antimony and antimony telluride in the system Sb–Sb_2Te_3(Eqs. 15 and 16, with $x_{Sb}+x_{Sb_2Te_3}=1$) and partial vapor pressure of antimony and tellurium telluride in the system Sb_2Te_3–Te (Eqs. 17 and 18, with $x_{Sb_2Te_3}+x_{Te}=1$) the boundaries of the liquid coexistence fields were calculated with the addition of the antimony-tellurium state diagram [18] by liquid–vapor phase transitions at atmospheric pressure (101.3 kPa) and in vacuum 0.9 kPa (Fig. 6). The pressure value of 0.9 kPa is due to the fact that lowering the pressure under the conditions of distillation processing of mattes represented by various chalcogenides below the specified value is not possible due to different boiling temperatures (partial values of saturated vapor pressure) of the latter.

$$\begin{aligned}\ln\overline{p}_{Sb} =&(21,720x^4_{Sb}-56,837x^3_{Sb}+53,298x^2_{Sb}\\&-26,722x_{Sb}-8,214+3,753\ln x_{Sb})\cdot T^{-1}\\&-10.68x^4_{Sb}+26.837x^3_{Sb}-23.312x^2_{Sb}\\&+10.502x_{Sb}+16.961-0.668\ln x_{Sb}\end{aligned} \quad (15)$$

$$\begin{aligned}\ln\overline{p}_{Sb_2Te_3} =&(21,720x^4_{Sb_2Te_3}-59,003x^3_{Sb_2Te_3}+58,172x^2_{Sb_2Te_3}\\&-22,462x_{Sb_2Te_3}-15,894)\cdot T^{-1}-10.68x^4_{Sb_2Te_3}\\&+30.123x^3_{Sb_2Te_3}-30.706x^2_{Sb_2Te_3}+12.095x_{Sb_2Te_3}\\&+22.731+\ln x_{Sb_2Te_3}\end{aligned} \quad (16)$$

$$\begin{aligned}\ln\overline{p}_{Sb_2Te_3} =&(6,874x^3_{Sb_2Te_3}-20,560x^2_{Sb_2Te_3}+20,198x_{Sb_2Te_3}\\&-23,979+300\ln x_{Sb_2Te_3})\cdot T^{-1}-9.302x^3_{Sb_2Te_3}\\&+24.652x^2_{Sb_2Te_3}-21.611x_{Sb_2Te_3}+29.824\\&+1.231\ln x_{Sb_2Te_3}\end{aligned} \quad (17)$$

$$\begin{aligned}\ln\overline{p}_{Te} =&(-6,874x^3_{Te}+10,373x^2_{Te}+176x_{Te}-17,983)\\&\cdot T^{-1}+9.302x^3_{Te}-17.207x^2_{Te}+6.721x_{Te}\\&+24.045+\ln x_{Te}\end{aligned} \quad (18)$$

It is obvious that the process of evaporation of alloys at the tellurium edge of the state diagram will be accompanied by the enrichment of the vapor phase with elemental tellurium and the accumulation of antimony telluride in the bottom residue. With a similar process of evaporation of antimony edge alloys of the state diagram, the vapor will be enriched with antimony telluride and antimony will accumulate in the distillation residue. When antimony is refined from tellurium impurities, there will be a sequential transfer into the vapor phase first of tellurium and then of antimony telluride. At the same time, the separation of elements and compounds into each separately is not possible due to the presence of each of the components in the vapor phase. Thus, under equilibrium conditions and atmospheric pressure (101.3 kPa) in a vapor over an alloy containing 24 at% (25.0 wt%) Te, 54.4 at% (55.6 wt%) Te and 45.6 at% (44.4 wt%) Sb; at a pressure of 0.9 kPa, 30.2 at% (31.3 wt%) Te and 69.8 at% (68.7 wt%) Sb in the form of antimony telluride.

The separation of antimony-tellurium alloys by distillation into elements at atmospheric pressure is difficult due to the high boiling points of antimony-based alloys. In a vacuum, it is fundamentally possible, but a significant number of "distillation-condensation" cycles will need to be repeated. It should also be noted that a decrease in pressure negatively affects the quality of separation of alloys—the width of the fields (L + V) decreases with temperature, which entails an increase in the number of cycles of evaporation of the alloy and re-evaporation of the condensate.

4 Conclusions

The search for environmentally friendly methods of processing raw materials is an urgent task in the metallurgical sector. One such method is the distillation process, carried out at low pressure in a sealed apparatus. As a rule, the behavior and distribution of components during the processing are judged by state diagrams with the boundaries of the coexistence of liquid and vapor marked on them.

Due to the lack of information about liquid alloys of the antimony–tellurium system, we determined the partial vapor pressures of the solution components of this system and calculated the boundaries of the coexistence fields of melt and vapor at atmospheric pressure (101.3 kPa) and in vacuum 0.9 kPa. A pressure of 0.9 kPa is the vacuum at which the vacuum distillation of industrial mattes is realized.

Based on the position of the obtained field boundaries (L + V) on the state diagram Sb–Te, the separation of antimony alloys with tellurium (particular system Sb–Sb_2Te_3) by distillation into individual components at atmospheric pressure is difficult due to the high boiling points of antimony-based alloys. In a vacuum, it will require a significant number of condensate re-evaporation cycles due to the small width of the fields of coexistence of melt and vapor in temperature. The process of separating antimony telluride and tellurium (particular system Sb_2Te_3–Te) is similar. However, in the case of the distillation processing of the chalcogenide melt, which occurs at 1150–1250 °C, tellurium and antimony telluride will be predominantly concentrated in the vapor phase and then in the condensate.

Based on the partial values of the vapor pressure of the components that make up the system, we calculated the thermodynamic functions of the formation and evaporation of liquid solutions. It was found, that the formation of alloys is accompanied by an increase in disorder in the system and proceeds mainly with the release of heat. However, up to about 12 at% Te in the alloy, the process of alloy formation is endothermic. The enthalpy of mixing has a minimum (-5.29 ± 0.36 kJ/mol) at 42.0 at% Te. However, an insignificant value of the exothermic effect indicates a weak interaction of unlike particles in a liquid bath.

The change in the integral entropy of mixing is sign-alternating in the concentration range from 60.0 to 70.6 at% Te. The formation of solutions is accompanied by an increase in disorder in the system with a function maximum (1.57 ± 0.17 J/(mol × K)); from 70.6 to 100 at% Te, some ordering of particles in the melt is observed with a function minimum (-2.37 ± 0.25 J/(mol × K)). The change in the enthalpy of mixing is negative over the entire range of existence of liquid alloys of the Sb_2Te_3–Te system with a minimum (-11.80 ± 1.27 kJ/mol) at 82.9 at% tellurium in solution. A noticeable negative value of the enthalpy of mixing is a sign of an exothermic process, accompanied by the interaction of unlike particles in the liquid phase.

Thus, in the study, the vapor pressure of the antimony-tellurium system components was determined for the first time in the entire range of element concentrations. Based on these data, the phase transition boundaries of the antimony-tellurium system, including three aggregate states (solid, liquid, and vapor), were calculated for the first time, and a complete phase diagram was constructed for the first time at atmospheric pressure (101.3 kPa) and in vacuum (0.9 kPa). The found boundaries of the coexistence fields of liquid and melt indicate the possibility of rare elements extraction: antimony and tellurium during the distillation processing of polymetallic mattes into sulfide condensate. Also, partial and integral functions of phases were determined for the first time in the entire range of component concentrations, which will replenish the physical and chemical databases, which is significant for technological calculations.

The obtained results are reference data and have theoretical and applied applications, including creating effective

technical solutions for improving the technology of extracting rare metals by vacuum distillation with their concentration in one intermediate product.

Acknowledgements The authors gratefully acknowledge the support extended by the Ministry of Science and Higher Education of the Republic of Kazakhstan for funding this research.

Author Contributions VV: Methodology, Data curation, Writing–original draft preparation, Project administration. ST: Conceptualization, Writing–original draft preparation. AN: Methodology, Investigation, Writing–review and editing, Visualization. XL: Investigation, Visualization. AT: Investigation.

Funding The work was supported by the Science Committee of the Ministry of Science and Higher Education of the Republic of Kazakhstan (Grant AP14869944).

Data Availability Data will be made available on request.

Declarations

Conflict of interest The authors declare that they have no conflict of interest.

References

1. S.M. Kozhakhmetov, S.A. Kvyatkovsky, M.K. Sultanov, Z.K. Tulegenova, A.S. Semenova, Kompleks. Ispolz. Mineral. Syra Comp. Use Min. Res. **306**, 54 (2018). https://doi.org/10.31643/2018/6445.17
2. Z. Wang, J. Gao, X. Lan, G. Feng, Z. Guo, Resour. Conserv. Recycl. **182**, 106316 (2022). https://doi.org/10.1016/j.resconrec.2022.106316
3. M. Chen, K. Avarmaa, P. Taskinen, L. Klemettinen, R. Michallik, H. O'Brien, A. Jokilaakso, Miner. Eng. **191**, 107969 (2023). https://doi.org/10.1016/j.mineng.2022.107969
4. N.K. Dosmukhamedov, E.E. Zholdasbay, Kompleks. Ispolz. Mineral. Syra Comp. Use Min. Res. **312**, 31 (2020). https://doi.org/10.31643/2020/6445.04
5. N.K. Dosmukhamedov, E.E. Zholdasbay, M.B. Kurmanseitov, AA Argyn, MA Zheldibay, Kompleks. Ispolz. Mineral. Syra Comp. Use Min. Res. **313**, 5 (2020). https://doi.org/10.31643/2020/6445.11
6. B.K. Kenzhaliev, S.A. Kvyatkovsky, S.M. Kozhakhmetov, L.V. Sokolovskaya, A.S. Semenova, Kompleks. Ispolz. Mineral. Syra Comp. Use Min Res. **306**, 45 (2018). https://doi.org/10.31643/2018/6445.16
7. F. Kukurugya, A. Rahfeld, R. Möckel, P. Nielsen, L. Horckmans, J. Spooren, K. Broos, Miner. Eng. **122**, 17 (2018). https://doi.org/10.1016/j.mineng.2018.03.030
8. N. Dosmukhamedov, A. Argyn, E. Zholdasbay, G. Moldabayeva, J. Mater. Res. Technol. **9**, 11826 (2020). https://doi.org/10.1016/j.jmrt.2020.08.029
9. S. Wang, Q. Wang, X. Guo, Q. Tian, S. Qu, Z. Wang, M. Huang, Trans. Nonferrous Met. Soc. China **32**, 4113 (2022). https://doi.org/10.1016/S1003-6326(22)66082-5
10. B.K. Kenzhaliyev, S.A. Kvyatkovskiy, M.A. Dyussebekova, A.S. Semenova, D. Nurhadiyanto, Kompleks. Kompleks. Ispolz. Mineral Syra Comp. Use Min. Res. **323**, 23 (2022). https://doi.org/10.31643/2022/6445.36
11. E. Kim, L. Horckmans, J. Spooren, K. Broos, K.C. Vrancken, M. Quaghebeur, Hydrometallurgy **169**, 290 (2017). https://doi.org/10.1016/j.hydromet.2017.02.007
12. D.H. Kim, S.K. Ko, J.H. Lee, C.W. Won, Met. Mater. **3**, 193 (1997). https://doi.org/10.1007/BF03025962
13. J. Lee, K. Kurniawan, K.W. Chung, S. Kim, Met. Mater. Int. **27**, 2160 (2021). https://doi.org/10.1007/s12540-020-00716-7
14. G.A. Flores, C. Risopatron, J. Pease, JOM **72**, 3447 (2020). https://doi.org/10.1007/s11837-020-04255-9
15. S. Sineva, M. Shevchenko, D. Shishin, T. Hidayat, J. Chen, P.C. Hayes, E. Jak, JOM **72**, 3401 (2020). https://doi.org/10.1007/s11837-020-04326-x
16. M. Nagamori, P.J. Mackey, Metall. Mater. Trans. B **9**, 567 (1978). https://doi.org/10.1007/BF03257205
17. V. Ettler, Z. Johan, C.R. Geosci. **335**, 1005 (2003). https://doi.org/10.1016/j.crte.2003.09.005
18. V.N. Volodin, R.A. Isakova, *Distillation Processes of Separation Sulfide and Metal Melts: Theory and Technology* (Tengri Ltd., Karaganda, 2015), p.260
19. T. Maekawa, T. Yokokawa, K. Niwa, J. Chem. Thermodyn. **4**, 873 (1972). https://doi.org/10.1016/0021-9614(72)90009-2
20. B. Predel, J. Piehl, M.J. Pool, Z. Metallkde. **66**, 388 (1975). https://doi.org/10.1515/ijmr-1975-660702
21. B. Predel, F. Gerdes, U. Gerling, Int. J. Mater. Res. **70**, 109 (1979). https://doi.org/10.1515/ijmr-1979-700210
22. C.L. Sullivan, J.E. Prusaczyk, K.D. Carlson, J. Chem. Phys. **53**, 1289 (1970). https://doi.org/10.1063/1.1674136
23. J. Bagdavadze, R. Chagelishvili, N. Gagnidze, A. Kandelaki, R. Rasmadze, Z. Tsikaridze, Bull. Georg. Nat. Acad. Sci. **7**, 75–79 (2013)
24. C. Shi, N. Li, W. Zhang, Int. J. Mater. Res. **112**, 373 (2021). https://doi.org/10.1515/ijmr-2020-7951
25. F.R. Aliyev, E.N. Orujlu, D.M. Babanly, Azer. Chem. J. **4**, 53 (2021). https://doi.org/10.32737/0005-2531-2021-4-53-59
26. V.N. Volodin, S.A. Trebukhov, B.K. Kenzhaliyev, A.V. Nitsenko, N.M. Burabaeva, Rus. J Phys. Chem. A **92**, 407 (2018). https://doi.org/10.1134/s0036024418030330
27. N.A. Ilyasheva, Inorg. Mater. **9**, 1677–1679 (1973)
28. E.T. Ibragimov, A.S. Shendyapin, V.N. Nesterov, RZh. Khobdabergenov, Proc. Inst. Metall. Ore Benefication Acad. Sci. KazSSR **52**, 61–65 (1977)
29. Y.H. Lee, K. Itagaki, Trans. JIM. **27**, 987 (1986). https://doi.org/10.2320/matertrans1960.27.987
30. V.N. Volodin, V.E. Khrapunov, R.A. Isakova, A.S. Shendyapin, S.A. Trebukhov, Bull. Nat. Acad. Sci. Repub. Kazakhstan **3**, 45–51 (2010)
31. Z. Dong, L. Li, H. Xiong, G. Liu, Y. Wang, Z. Zhou, B. Xu, B. Yang, Vacuum **201**, 111067 (2022). https://doi.org/10.1016/j.vacuum.2022.111067
32. H. Kametani, C. Yamauchi, K. Murao, M. Hayashida, Trans. JIM **14**, 218 (1973). https://doi.org/10.2320/matertrans1960.14.218
33. A. Allaire, R. Harris, Metall. Trans. B **20**, 793 (1989). https://doi.org/10.1007/BF02670185

34. Z. Zhou, D. Liu, H. Xiong, C. Wang, B. Ma, L. Wei, Y. Chen, K. Huang, Vacuum **188**, 110172 (2021). https://doi.org/10.1016/j.vacuum.2021.110172
35. K.J. Singh, R. Satoh, Y. Tsuchiya, J. Phys. Soc. Jpn. **72**, 2546 (2003). https://doi.org/10.1143/JPSJ.72.2546
36. N.P. Lyakishev (ed.), *State Diagrams of Binary Metal Systems: Directory*, vol. 3, book 2, (Mashinostroenie, Moskow, 2000), p. 448
37. C. Guo, C. Li, Z. Du, J. Electron. Mater. **43**, 4082 (2014). https://doi.org/10.1007/s11664-014-3299-7
38. J.B. Clark, P.W. Richter, Proc. 7 th Int. AIRAPT Conf. (Pergamon Press, Oxford, 1980), pp. 363–371
39. V.N. Volodin, *Physical Chemistry and Technology of Cadmium Refining* (Print-S, Almaty, 2011)
40. D.M. Chizhikov, N.N. Sevryukov, News Acad. Sci. USSR Dep. Eng. Sci. **9**, 89–97 (1941)
41. Yu.V. Tsvetkov, V.M. Edelstein, J. Ap. Chem. **35**, 1927–1933 (1962)